AIAA'87

AIAA-87-2021

Liquid Propellant Tank Ullage Bubble Deformation and Breakup in Low Gravity Reorientation

J.J. Der and C.L. Stevens, The Aerospace Corp., Los Angeles, CA

AIAA/SAE/ASME/ASEE 23rd Joint Propulsion Conference

June 29-July 2, 1987/San Diego, California

LIQUID PROPELLANT TANK ULLAGE BUBBLE DEFORMATION AND BREAKUP IN LOW GRAVITY REORIENTATION

James J. Der* and Christine L. Stevens**
The Aerospace Corporation, Los Angeles, CA 90009

Abstract

Collapse, geyser formation, and breakup of a reorienting ullage bubble in liquid propellant tanks under low gravity have been studied numerically. The response of liquid propellant in a partially filled spacecraft tank under a suddenly imposed external acceleration has been examined. The similitude variables we developed in a previous paper for correlating unsteady numerical and experimental data of the bubble motion are applicable here for the kinetics of the bubble surface. When the bubble is initially situated further from the new top surface, some of the energy is dissipated in fragmenting the bubble. Also, there is more liquid between the bubble and the wall. Thus, the further the initial location of the ullage is from the new top, the weaker the liquid jet striking the wall. For the case of larger ullage, there is less liquid participation in the geyser formation, and the jet is therefore weaker. With an ullage as large as 30%, the geyser can at most barely penetrate the bubble.

Introduction

In operations of liquid propellant spacecraft, low-g fluid mechanics is involved during the maneuvering of the vehicles. Problems arising in spacecraft connected with low-g fluid mechanics include tank sloshing in orbital-transfer-vehicles (OTV), propellant management and handling in OTVs and space stations, fluid transfer from vehicle to vehicle and between a vehicle and a space station, and operations such as satellite refueling and propellant scavenging.

Because the mass of the contained liquids can be a substantial portion of that of the entire vehicle, the motion of these fluids can significantly affect the dynamics of the vehicle. In the ejection of an OTV from a space shuttle, for example, the ullage motion may induce a significant lateral force on the vehicle. The effects of the ullage reorientation on the external vehicle dynamics was studied in Reference 1.

In our previous study of the reorientation of the ullage, we found that the bubble deformed significantly as the ullage repositioned itself under an external acceleration. For conditions corresponding to the relatively high Bond numbers typically experienced in orbital vehicles, the bubble forms a geyser, collapses, and breaks into smaller bubbles. Such phenomena occur independent of the initial bubble location, including the case with the bubble initially located exactly at the new top. (New top is the new equilibrium position for the bubble under the external acceleration.) Plesset (Reference 2) and others have shown that the bubble deformation significantly affects the wall structure of the propellant tank by striking the tank surface with a high velocity jet. In addition, the breakup of the bubble may further affect acquisition, refilling, venting, mixing, and other propellant management operations. It is important, therefore, to study the conditions leading to bubble collapse or breakup, and those conditions that result in the geyser striking the container wall.

In the present study, we focus on the following questions: (1) With an ullage initially located adjacent to the tank wall, for what size (in percent volume) ullage will the jet from the geyser strike the tank surface? (2) How does the initial distance of the ullage from the wall affect the probability of the geyser striking the surface?

Discussion

The fluid mechanics problem is complex because it is unsteady, three-dimensional in nature, and involves gravity forces, free surfaces between ullage and liquid, and surface tension. These factors are in addition to the more common phenomena, such as effects of viscosity and inertia, encountered in fluid mechanics.

Geometry and Boundary Conditions

Propellant tanks come in a variety of shapes and sizes. Following Reference 1 in exploring a propellant tank of nominal size and shape closely resembling those used in spacecraft, a spherically shaped tank 1 meter in radius will be studied. The geometry of the propellant ullage in such a tank is depicted in Figure 1. With the ullage positioned as shown in Figure 1, an external acceleration in the indicated direction results in the ullage reorienting (re-locating) itself to the new top.

Similarity Group Parameters and Normalized Variables

A simple dimensional analysis of the physical variables yielded the pertinent dimensionless groups for this problem. These parameters include the Reynolds (Re), Froude (Fr), and Bond (Bo) numbers, and the ratios of densities (R_ρ) and viscosities (R_μ) of the ullage to those of the liquid. They are defined by the following relations:

*Member of the Technical Staff, Fluid Mechanics Dept., Vehicle and Control Division
**Member of the Technical Staff, Engineering Analysis Programming Dept., Information Processing Division

$$Re = \rho v r/\mu \qquad Fr = v/(ar)^{1/2}$$

$$Bo = \rho a r^2/\sigma$$

$$R_\rho = \rho_u/\rho \qquad R_\mu = \mu_u/\mu$$

Here ρ is the fluid density, v the ullage velocity, r the tank radius, μ the fluid viscosity, a the external acceleration, and σ the fluid surface tension. Fluid properties without subscript pertain to the liquid, and those with subscript u pertain to the ullage.

The values of R_ρ and R_μ are normally small for ullage consisting of liquid vapor or other gases. Matching these two parameters for the model with those of the prototype is relatively easy when liquid-gas (or liquid-vapor) combinations are used for the modeling fluids. When bi-liquid modeling techniques (simulating low Bond number condition by using two liquids of nearly the same density) are used, however, these two ratios will not be closely matched. The consequence of not matching these two parameters will be the subject of a future study.

Fluid Properties

Liquid propellants used in spacecraft include cryogenic fluids such as liquid hydrogen and liquid oxygen. Storable propellants for space applications include hydrazine, unsymmetrical dimethylhydrazine (UDMH), and nitrogen tetroxide. In addition, water has been accepted as a test fluid for subscale model low-g fluid dynamic experiments conducted for the space shuttle. The properties of the liquids are as follows:

Liquid	ρ kg/m^3	ρ/μ 10^{-6} m^2/s	σ/ρ 10^{-4} m^3/s
Hydrazine	1009.0	0.965	0.748
Liquid hydrogen	72.8	0.00223	0.33
Liquid oxygen	1140.0	0.167	0.116
Nitrogen tetroxide	1450.0	0.237	0.19
UDMH	791.0	0.741	0.254
Water	995.0	1.01	0.728

With these fluids, and propellant tanks of representative size, the Bond number should be greater than 10 and the Reynolds number greater than 1000. The viscous effects should be small, and the surface tension should also be small until the bubble breaks up into smaller ones.

Normalized Variables

For the purpose of correlating the physical phenomena for different tank sizes under various levels of acceleration, we have developed non-dimensional variables defined by the following relations:

$$t = t^* \cdot (r/a_c)^{1/2} \tag{1a}$$

$$x_i = x_i^* \cdot r \tag{1b}$$

$$v_i = v_i^* \cdot (a_c r)^{1/2} \tag{1c}$$

$$p = p^* \cdot \rho a_c r \tag{1d}$$

where the starred values are the normalized quantities, ρ is the fluid density, r is the tank radius, a_c is the characteristic acceleration (e.g., the maximum external acceleration), v_i's are the liquid velocities in the directions of the coordinates x_i's, and p is the fluid pressure.

In terms of the starred quantities, the flow equations become

$$\partial v_i^*/\partial x_i^* = 0 \tag{2a}$$

$$\partial v_i^*/\partial t^* + v_j^* \cdot \partial v_i^*/\partial x_i^* = \partial p^*/\partial x_i^* + f_i^*(t^*) \tag{2b}$$

where $f^*_i(t^*) = f_i(t)$. The quantity $f_i(t)$ is the external acceleration in the x_i direction divided by a_c. Thus the flow field is invariant in terms of the starred quantities as long as the $f^*_i(t^*)$ are kept the same.

An example where the $f_i^*(t^*)$ are similar is the case of constant acceleration. Another case of external acceleration that can easily be made similar consists of pulses, with the time period of each pulse for the model selected so that, in terms of the starred time, it is equal to that of the prototype. Other variations of the external acceleration can be made, but they may be somewhat harder to execute in practice.

Numerical Simulation

The computer program used for numerical simulation is the HYDR-3D code. This code, developed by Flow Science Inc., is a finite-difference code that solves the unsteady three-dimensional Navier-Stokes equations. It can handle incompressible viscous fluids with the inclusion of free surfaces, surface tension, and gravity. This code uses variable spacing on a rectangular (Cartesian or cylindrical) grid with curved boundaries taken into account by a "volume fraction" method employing piecewise linear boundary geometry. The code has a control logic for time-step size selection to assist maintenance of accuracy and elimination of numerical instabilities. It can handle both small and large ullage volumes. The algorithm, an improved version of the SOLA-VOF developed by Nichols et al. (Reference 3), is second-order accurate inside the flow field and first-order accurate on the boundaries. The modeling of the surface tension is marginal and is not expected to yield more than qualitative results when capillary effects are significant. For the present application, however, we can neglect the surface tension aspect except when the bubbles break into very small pieces. The HYDR-3D code has seen limited testing by Aydelott, et al. (Reference 4) for low-g bubble dynamics computations. While we expect that this code will render a reasonable simulation of the physical phenomena, more verification, such as the experiment to be conducted in the space shuttle, will be needed.

Ullage Motion

Our main interest in this study is the motion of the surface of an ullage reorienting in a propellant tank upon experiencing an external acceleration. This case should be representative of the ullage motions commonly encountered in spacecraft propellant tanks. A 14 x 14 cell-net is used in the x-y plane. Symmetry is assumed between positive and negative z, with eight cells used for each half. Cases of coarser grid (12 x 12 x 8 and 10 x 10 x 8) have been computed to test the sensitivity of the cell size. The net size adopted appears to be adequate until the bubble fragments, at which point the resolution of the smaller bubbles is marginal at best.

The bubble is assumed to be initially at rest and takes the shape of a sphere (corresponding to zero gravity). A 20% volume ullage is considered for the nominal case. The motion for ullage with initial positions at several locations along the line between the new bottom (180° from the new top) and the new top have been analyzed. Also analyzed is the effect of bubble size from 10 to 60% ullage volume. The results are discussed below.

Figure 2 shows the time sequence of the bubble cross section on the symmetry plane for a 20% ullage initially located in the new top. This is the position for which we expect the geyser formation to be the least pronounced. The new equilibrium shape of the bubble is somewhat flattened. The amount of flattening depends on the magnitude of the Bond number (References 5 and 6). As it began to reorient, the ullage immediately started to deform, because of the action of the liquid. As the deformation proceeds, the liquid near the wall pushes the bubble on the backside, particularly near the center of the bubble surface, causing a geyser to form. The geyser eventually strikes the tank wall. Such geyser formation of the ullage is absent in the case of a bubble rising in a long tube, and is due to the interaction between the bubble and the fluid and the proximity of the wall in the path of the bubble motion.

In the case we have just discussed, the bubble is initially positioned immediately adjacent to the new top--the tank surface the geyser will strike. In this case, the geyser has the shortest distance to accelerate before impact. When the initial position of the ullage is further away, the geyser has more room to accelerate, and thus may impact the tank surface with higher velocity. Figure 3 presents the time sequence of a bubble initially situated at the center of the tank. Figure 4 presents the time sequence of the bubble initially situated adjacent to the new bottom--the opposite side of the new top surface. In each case the bubble splits before the geyser reaches the tank surface; thus, there is a layer of liquid cushioning the liquid jet.

Figures 5a and 5b, respectively, show the location and velocity time histories of the centroid of the ullage. For the case with the bubble initially adjacent to the new top, the centroid of the ullage reached as close to the new top as it could at about 1.5 sec and was actually retreating when the geyser leading edge struck the tank surface. For the other two cases, with the initial ullage positions further away from the impact surface, the ullage centroid did not reverse in direction, but did slow down. This deceleration of the centroid should affect the advancement of the geyser.

In Figure 6, the locations of the geyser leading edge for the 20% ullage at various initial positions are presented. For the case with the ullage initially adjacent to the new bottom (case b) the leading edge of the geyser attains a higher speed than for the case with the ullage initially adjacent to the new top (case a). But this higher speed appears to be diminished as the geyser approaches the new top, and the bubble splits with a liquid layer of more than 25% of the tank radius between the geyser leading edge and the tank surface. For the intermediate case, with the ullage initially at the tank center (case c), the velocity of the geyser leading edge is nearly the same as that of case a most of the time until it encroaches on the tank surface. At this point the action of the liquid layer between the bubble and the new top causes the geyser to slow down just before the bubble splits. Thus the cushioning effects are evident.

A somewhat analogous variation from the nominal case (20% ullage initially adjacent to the new top) is the following: With a larger ullage, since there is more space for the geyser to accelerate, would there actually be more of a tendency to strike the tank surface? This, of course, cannot be true for a very large ullage, since there will not be sufficient liquid to penetrate the bubble. Figure 7, in which the time sequence for the case of a 30% ullage is presented, shows that the geyser in that case did indeed fail to penetrate the bubble. Figure 8, however, shows that for the case of a 40% ullage the geyser does penetrate the bubble and strike the surface, although just barely. Computations for these and other ullage sizes (10, 35, 45, 50, and 60%) not shown, indicate that for ullages of 30% or larger, only at nearly 40% will the geyser penetrate the bubble.

A possible explanation for how the geyser in the 40% ullage case is able to penetrate the bubble is as follows. Two factors control the penetration of the bubble by the geyser: the amount of liquid behind the geyser (which favors smaller ullage), and the distance available for the geyser to accelerate (which favors larger ullage). For ullage close to 40% there apparently is a near balance between these mechanisms, i.e., at 40% there is a crossover between these two factors (thus from near miss to barely strike). Note that such a small margin may be close to the margin of error of the numerical computations. This tentative explanation will be examined in more detail in a future study. Such a study will be conducted by means of increased computational accuracy and possibly in conjunction with an investigation of forces exerted by the geyser impacting the surface (as discussed below).

Figures 9a and 9b present the location and velocity time histories of the ullage centroid. Figure 10 presents the location time histories of the geyser leading edge for 20, 30, 40, and 50% ullage. It appears that at 40%, the increased distance available for acceleration allows the geyser to penetrate the bubble, even only barely, and for ullage larger than this small range of size near 40%, the lack of liquid participating in the geyser action prevents it from reaching the other side of the bubble.

For ullage smaller than 30%, the geyser appears to always succeed in impacting the tank surface based on the present computation. However, we were using a rather coarse grid, and computation for ullage smaller than 20% may not be sufficiently accurate to draw quantitative conclusions. The computed results for ullage smaller than 20%, however, indicate that until the ullage is so small that surface tension effects become important, small ullage most likely will collapse and the geyser is likely to strike the tank surface.

It would be interesting to see, quantitatively, the effects of the geyser impact on the surface. This would involve the detailed mapping of the pressure on the struck surface. Such an effort requires more accurate and detailed computations than we are currently conducting. A minor amount of code modification is also required to integrate the local forces on the surface in the neighborhood of the point of impact of the geyser. This will be a subject of a future effort.

Conclusions

Deformation and breakup of an ullage bubble in liquid propellant tanks under low gravity was studied numerically. It was found that the further the initial ullage location is from the new top, the weaker is the liquid jet striking the wall. The liquid jet weakens because of the energy expended in breaking up the collapsing bubble and the cushioning effects of the liquid layer between the bubble and the struck tank surface. It appears that around 40%, the increased acceleration space allows the geyser to barely penetrate the bubble, and for ullage larger than this small range of size near 40%, the lack of liquid participating in the geyser action prevents it from reaching the other side of the bubble. With an ullage nearly 30% or larger, the geyser can at most barely penetrate the bubble. For ullage smaller than 30%, but not so small that surface tensions become important, the computed results indicate that the bubble most likely will collapse and the geyser strike the tank surface.

Acknowledgment

This work was supported by the U. S. Air Force Space Division under Contract No. F04701-85-C-0086-P00016.

References

1. Der, J. and C. Stevens, "Low-Gravity Bubble Reorientation in Liquid Propellant Tanks," AIAA Paper 87-0622, presented in the AIAA 25th Aerospace Science meeting, Reno, Nevada, 5-7 January 1987.

2. Plesset, M. and R. Chapman, "Collapse of an Initially Spherical Vapor Cavity in the Neighborhood of a Solid Boundary," Journal of Fluid Mechanics (1971), Vol. 47, Part 2, pp. 283-290.

3. Nichols, B. et al. "SOLA-VOF: A Solution Algorithm for Transient Fluid Flow with Multiple Free Boundaries," Los Alamos Scientific Laboratory Report LA-8355, 1980.

4. Aydelott, J., et al. "NASA Lewis Research Center Low-Gravity Fluid Management Technology Program," NASA Technical Memorandum 87145, 4 November 1985.

5. Salzman, J., "Low-Gravity Liquid-Vapor Interface Configurations in Spherical Containers," NASA-LeRC, TN D-5648, February 1970.

6. Hasting, L. and R. Rutherford III, "Low Gravity Liquid-Vapor Interface Shapes in Axisymmetric Containers and a Computer Solution," NASA-MSFC, TM X-53790, October 1968.

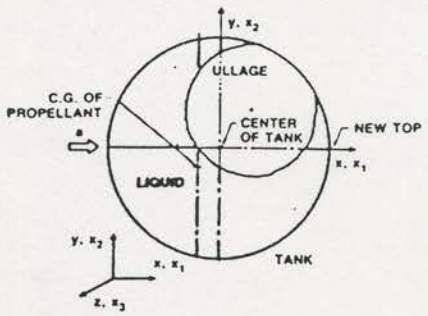

Figure 1. Low-g Ullage in a Liquid Propellant Tank

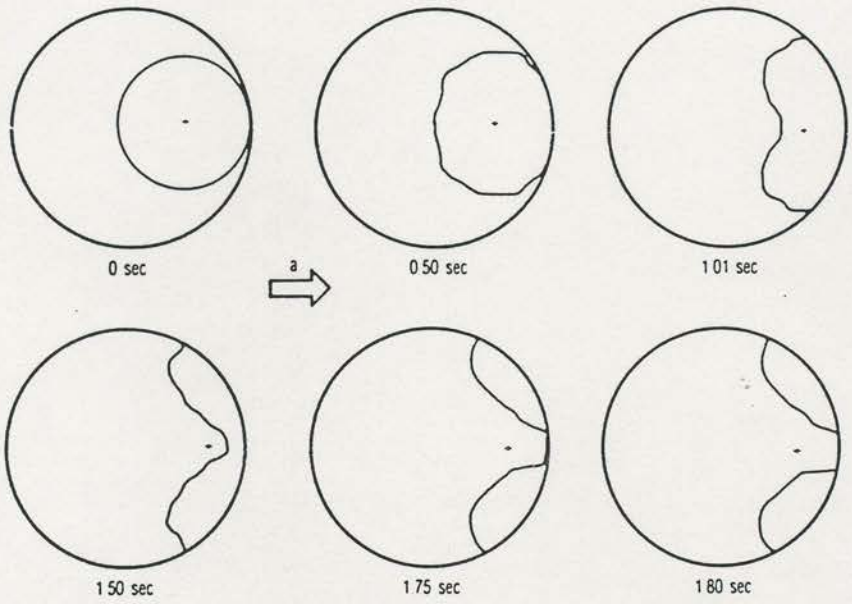

Figure 2. Time Sequence of a 20% Ullage Bubble Initially Located Adjacent to the New Top

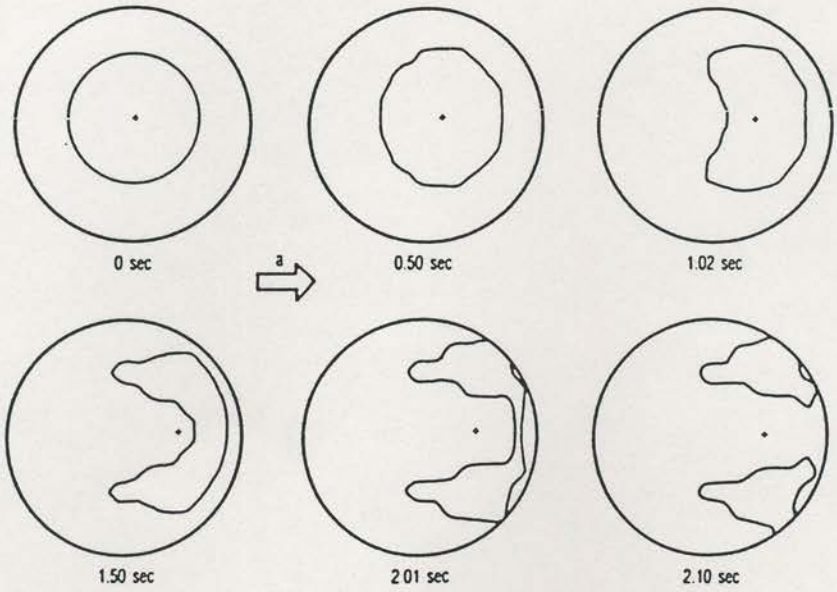

Figure 3. Time Sequence of a 20% Ullage Bubble Initially Located at the Tank Center

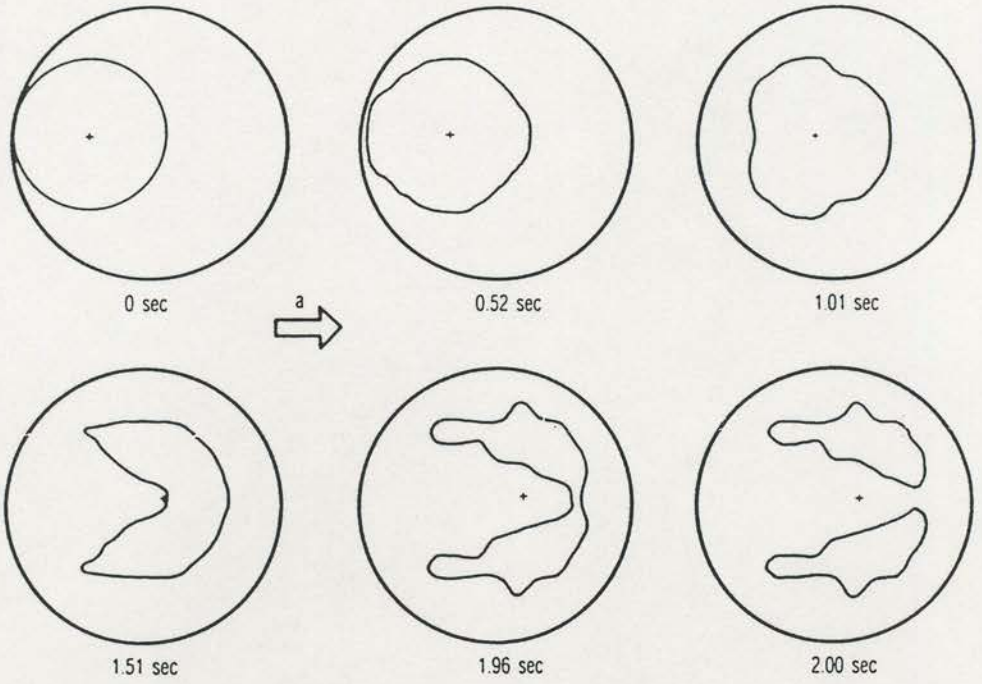

Figure 4. Time Sequence of a 20% Ullage Bubble Initially Located Adjacent to the New Bottom

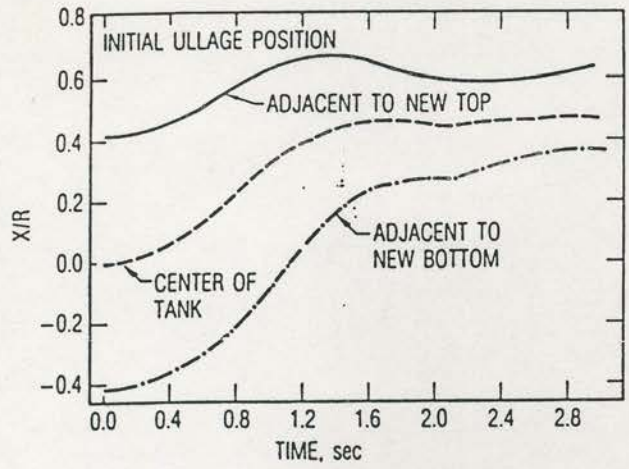

Figure 5a. Location Time Histories of Ullage Centroid for Various Initial Ullage Positions

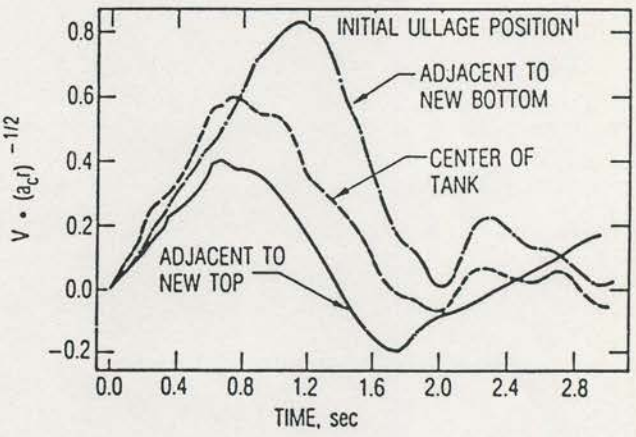

Figure 5b. Velocity Time Histories of Ullage Centroid for Various Initial Ullage Positions

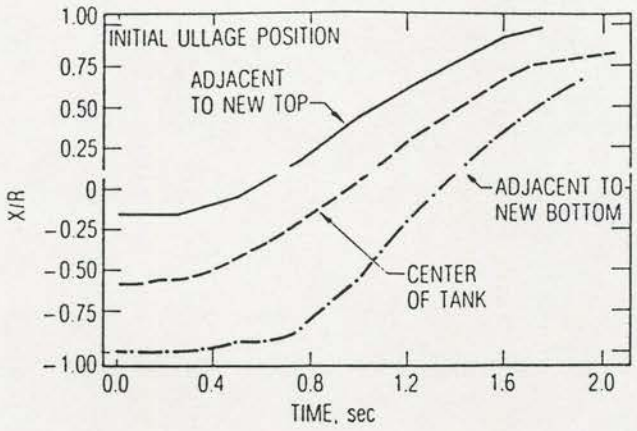

Figure 6. Geyser Leading Edge Location Time Histories for Various Initial Ullage Locations

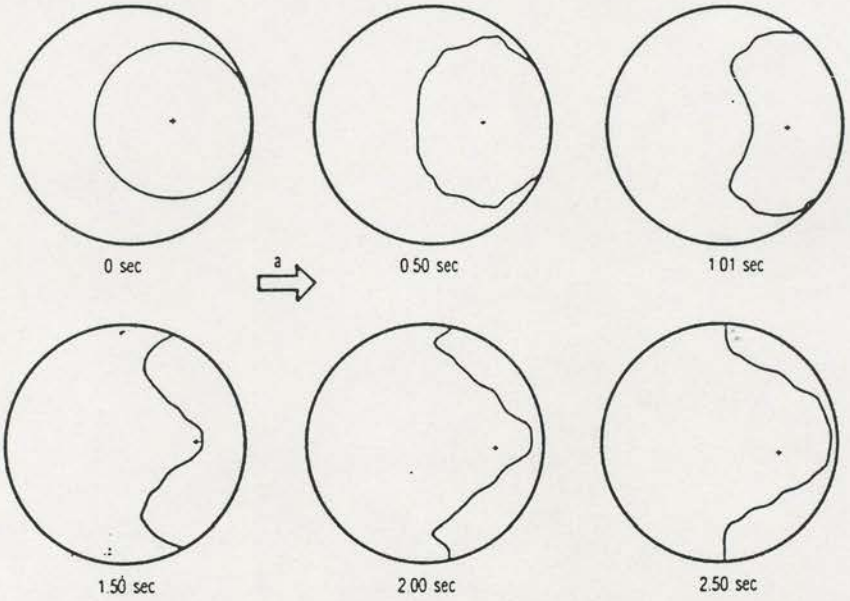

Figure 7. Time Sequence of a 30% Ullage Bubble Initially Located Adjacent to the New Top

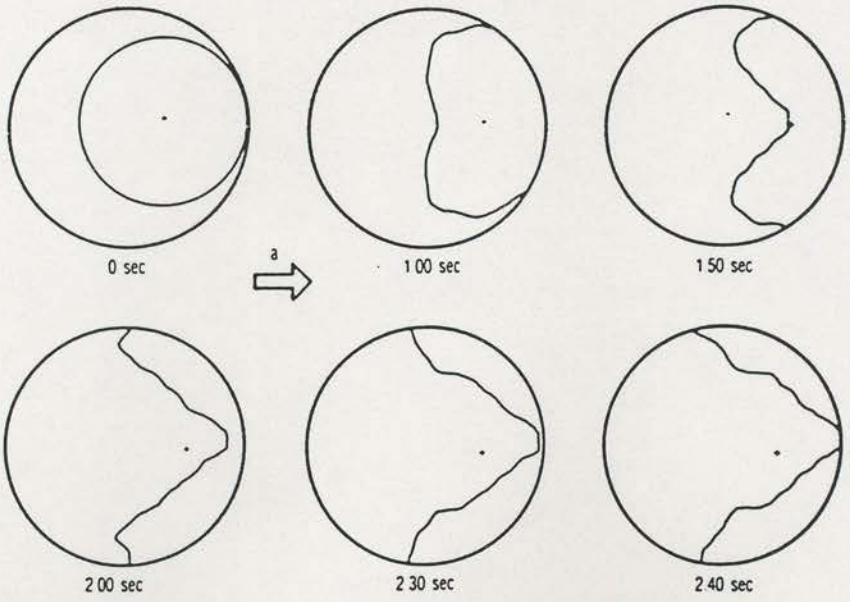

Figure 8. Time Sequence of a 40% Ullage Bubble Initially Located Adjacent to the New Top

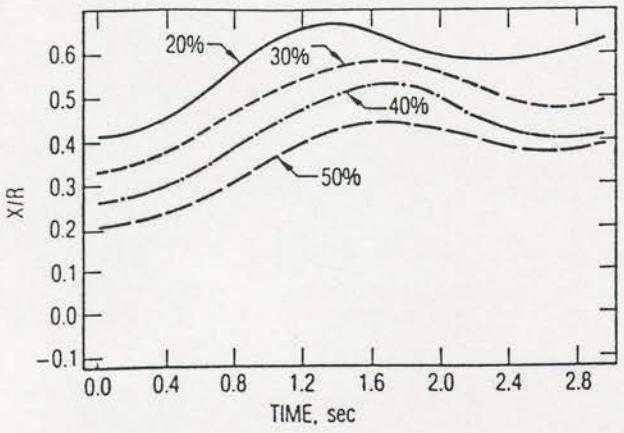

Figure 9a. Location Time Histories of Ullage Centroid for Various Ullage Sizes

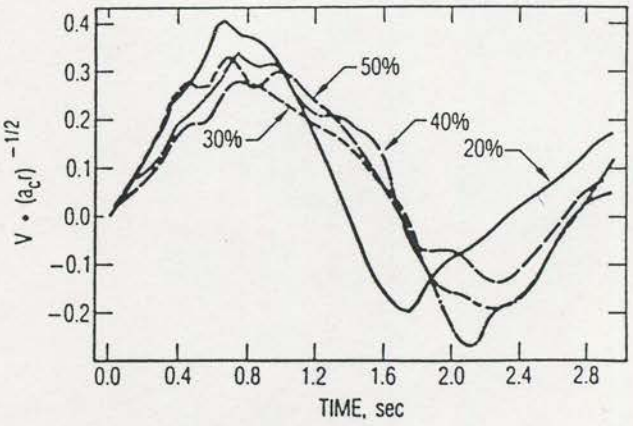

Figure 9b. Velocity Time Histories of Ullage Centroid for Various Ullage Sizes

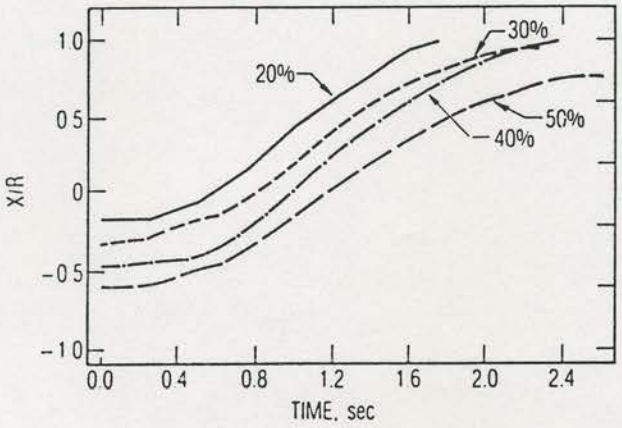

Figure 10. Geyser Leading Edge Location Time Histories for Various Ullage Sizes